PAPER • OPEN ACCESS

Towards field-effect controlled graphene-enhanced Raman spectroscopy of cobalt octaethylporphyrin molecules

View the article online for updates and enhancements.

Towards field-effect controlled graphene-enhanced Raman spectroscopy of cobalt octaethylporphyrin molecules

Stephan Sleziona[1,*] ⬤, Simon Rauls[1], Tobias Heckhoff[1], Leonard Christen[1], Erik Pollmann[1] ⬤, Lukas Madauß[1] ⬤, Steffen Franzka[2], Axel Lorke[1] ⬤, Heiko Wende[1] ⬤ and Marika Schleberger[1,*] ⬤

[1] Faculty of Physics and CENIDE, University of Duisburg-Essen, Lotharstrasse 1, Duisburg D-47057, Germany
[2] ICAN, University of Duisburg-Essen, Lotharstrasse 1, Duisburg D-47057, Germany

E-mail: stephan.sleziona@uni-due.de and marika.schleberger@uni-due.de

CrossMark

Abstract

During the last decade graphene-enhanced Raman spectroscopy has proven to be a powerful tool to detect and analyze minute amounts of molecules adsorbed on graphene. By using a graphene-based field-effect device the unique opportunity arises to gain a deeper insight into the coupling of molecules and graphene as graphene's Fermi level can be controlled by the transistor`s gate voltage. However, the fabrication of such a device comes with great challenges because of contaminations stemming from processing the device inevitably prevent direct adsorption of the molecules onto graphene rendering it unsuitable for field-effect controlled graphene-enhanced Raman spectroscopy measurements/experiments. In this work, we solve this problem by establishing two different fabrication procedures for such devices, both of which are in addition compatible with large area and scalable production requirements. As a first solution, selective argon cluster irradiation is shown to be an efficient way to remove resist residues after processing. We provide evidence that after the irradiation the enhancement of the molecular Raman signal can indeed be measured, demonstrating that this procedure cleans graphene's surface sufficiently enough for direct molecular adsorption. As a second solution, we have developed a novel stacking method to encapsulate the molecules in between two graphene layers to protect the underlying graphene and molecular layer from the harsh conditions during the photolithography process. This method combines the advantages of dry stacking, which leads to a perfectly clean interface, and wet stacking processes, which can easily be scaled up for large area processing. Both approaches yield working graphene transistors with strong molecular Raman signals stemming from cobalt octaehtylporphyrin, a promising and prototypical candidate for spintronic applications, and are therefore suitable for graphene based molecular sensing applications.

Supplementary material for this article is available online

(Some figures may appear in colour only in the online journal)

---

* Authors to whom any correspondence should be addressed.

1. Introduction

Shortly after the discovery of graphene in 2004 [1] Raman spectroscopy has proven to be a powerful tool for the characterization of graphene by offering the opportunity to

determine e.g. the layer number [2], doping [3] and defect density [4] in a fast and non-destructive way. Moreover in 2010 it was shown, that Raman spectroscopy is not just suitable to characterize graphene itself, but also that various molecules display a huge enhancement of their respective Raman signals when adsorbed onto graphene [5]. Utilizing graphene as a substrate in this so-called graphene-enhanced Raman scattering (GERS) [6] has many advantages, like a cleaner vibrational information [7], better control of molecular orientation [8] and a high reproducibility [9] compared to traditional substrates used for surface-enhanced Raman scattering (SERS), which are based on rough surfaces of noble metals, such as Ag or Au [10]. For SERS it is widely agreed on, that two mechanisms are responsible for the enhancement effect. The first one is called the electromagnetic mechanism (EM), where the local electromagnetic field is enhanced around metallic nanostructures placed on the otherwise inactive substrate [11–13]. The EM is thus plasmonic in nature and can reach an enhancement of up to 10^8 or even more [14, 15]. The second one is the so-called chemical mechanism (CM), which is not very well understood but generally attributed to the chemical interaction between the adsorbate and the substrate [16] and reaches enhancements of typically 10–10^2 [17]. For graphene the experimental data suggests that the CM is responsible for the observed Raman enhancement [5, 8, 18–20] while the EM is generally ruled out because the plasmon frequency of graphene is not located in the visible part of the spectrum [21]. The exact nature of the chemical mechanism has remained elusive and therefore GERS offers a unique opportunity to further investigate the details, e.g. by modulating the Raman enhancement via tuning the Fermi level in a graphene field-effect transistor (G-FET) [22–24]. Furthermore, in this transistor geometry GERS offers the opportunity to study the coupling of molecules and graphene in a non-destructive way and with unprecedented sensitivity down to a submonolayer amount of adsorbed molecules. In particular, in the field of molecular spintronics this kind of insight and additional control offered by GERS would thus present a major step forward. However, the successful exploitation of GERS in conjunction with such a system brings up severe challenges: processing graphene into a device inevitably leads to the introduction of defects into graphene and contaminations which are difficult to remove and which hinder molecular adsorption. The latter is in particular true if scalable fabrication processes such as photolithography and chemical vapour deposition (CVD) are used.

In this paper we address these challenges and present two alternative solutions, one based on an advanced post-processing step, the other on a novel pre-processing step. As a prototypical system we use cobalt octaethylporphyrin (CoOEP) as an interesting candidate for molecular spintronics [25–28] which has already been reported to exhibit a field dependent switching of its magnetic moment on graphene [29]. We begin with CoOEP molecules adsorbed on exfoliated graphene and show that Raman scattering from these CoOEP molecules can be detected down to submonolayer coverage of the molecules. In contrast, no CoOEP Raman

signals can be measured, when the molecules are evaporated onto the graphene surface after the field-effect transistor processing via photolithography. The photoresist residues seem to block the direct adsorption of molecules onto graphene, preventing the charge transfer and any Raman enhancement. Our whole fabrication procedure aims at large area samples compatible with mass fabrication. Therefore, as a first solution to efficiently remove the residual lithography resist we irradiate the transistors after the photolithography process with a mass-selected Ar cluster ion beam, which is a well-established tool for industrial scale applications [30], and demonstrate that after a subsequent molecule evaporation step, Raman enhancement of the molecules can indeed be measured again. As a second solution we shield the delicate molecular layer from the detrimental influence of the lithography process via our novel stacking method: before the lithography steps take place we fabricate a graphene/CoOEP/graphene heterostructure by transferring a second, protective CVD graphene layer on top of the graphene base layer onto which CoOEP molecules have been adsorbed. Thus, both, the graphene base layer and the CoOEP molecules are protected from the harsh conditions during the photolithography process. This method has several advantages compared to traditional stacking methods: Dry stacking suffers from the poor scalability of the process rendering it unsuitable for large scale industrially relevant applications while typical wet-transfer methods do come with the disadvantage of utilizing a polymer layer for stabilization. As will be discussed these residues cannot be fully removed by i.e. standard solvents and removers which is a big drawback regarding molecular sensing devices. Our novel method combines the advantages of providing a clean interface (like the dry stacking method) while being a scalable process (like the wet transfer processes). A clearly enhanced Raman signal is detected after the transfer of the top layer which persists even after the lithography processing has been completed. Both approaches yield functional devices which display the typical behaviour of a p-doped graphene transistor. We thus demonstrate that with the fabrication protocols successfully established in this work field-effect controlled graphene-enhanced Raman spectroscopy of CoOEP (and other similar) molecules becomes feasible.

2. Methods

Exfoliated graphene was prepared by mechanical exfoliation of Graphenium flakes (NGS Naturgraphit) onto a standard 285 nm SiO_2/Si substrate (Graphene Supermarket) wafer under ambient conditions. The fabrication process of the graphene transistors starts with the transfer of CVD graphene, grown on a copper substrate which is etched in an ammonium persulfate (APS) solution. The CVD graphene on a 6×6 inch copper wafer is bought from ACS Material and cut into 1×1 cm^2 squares for all the transfer steps. The procedure does not impose any principal limit on the sample size. Because we use large area CVD graphene, our approach is compatible with mass production [31] so that it may become attractive for

commercial applications such as molecular sensing devices based on graphene. Despite efforts to grow graphene onto other substrates copper is still mostly used for the growth of CVD graphene because of the low solubility of the carbon atoms in copper which leads to a self-limiting surface-catalyzed process [32].

After replacing the acid with water, the graphene sheet floating on the fluid was transferred onto a SiO_2/Si substrate with a oxide thickness of 285 nm by simply scooping it out. We want to emphasize that the whole transfer process is done without any supporting layer to stabilize the graphene. A detailed explanation for this method has been published elsewhere [33]. In a first photolithography step the large area CVD graphene was structured to eight graphene channels using an oxygen plasma. These graphene channels were contacted in a second photolithography step by depositing 10 nm Ti via electron beam evaporation and 70 nm Au by thermal evaporation. The photoresists were always removed in a bath of acetone at 60 °C. The same procedure was used to prepare the transistors based on the graphene/CoOEP/graphene heterostructure.

The CoOEP molecules were purchased from Porphyrin Systems and deposited by thermal vapor deposition in a ultra high vacuum chamber (base pressure $\leqslant 10^{-8}$ mbar). The amount of molecules evaporated was calculated utilizing a quartz crystal balance. We evaporated $5 \cdot 10^{-11}$ mol cm^{-2} onto the exfoliated graphene sample, which corresponds to less than one monolayer of molecules, even assuming that all evaporated molecules reach the sample and the sticking coefficient is one. This amount was chosen to demonstrate the high sensitivity of the Raman enhancement of CoOEP molecules on graphene. Onto all graphene field-effect devices 10^{-10} mol cm^{-2} of molecules were evaporated which would correspond to two layers of molecules assuming the same conditions as described above.

For the electrical characterization of the irradiated graphene transistor we applied a constant current of $I_{DS} = 10 \, \mu A$ between the drain and the source contact of the device, measured the modulation of V_{DS} by the backgate voltage and calculated the conductivity for the device. The backgate voltage was applied at the conducting silicon base of the SiO_2/Si substrate. For the electrical characterization of the graphene/CoOEP/graphene transistor we applied a constant voltage of $V_{DS} = 20 \, mV$ between the drain and the source contact, measured the variation of the drain source current (I_{DS}) with varying backgate voltage which was also applied at the conducting silicon base of the substrate and calculated the conductivity for the device.

The Raman spectra were recorded with a Renishaw InVia Raman-microscope at the Interdisciplinary Center for Analytics on the Nanoscale (ICAN) of the University of Duisburg-Essen (user operation). The excitation wavelength was 532 nm and the laser was focused onto a spot size of 1 μm using an objective with a numerical aperture of 0.85. The laser power was adjusted to 0.4 mW to avoid heating effects in graphene as well as thermal decomposition of the molecules.

Atomic force microscopy (AFM) images were obtained with a Bruker Dimension Icon at the Interdisciplinary Center of Analytics on the Nanoscale (ICAN) of the University of Duisburg-Essen by using a variation of the conventional tapping mode, i.e. the so-called Peakforce Tapping mode with RTESPA-300 tips. This mode allows for a better control over the force between tip and sample and thus gives improved control over tip induced modifications of the surface.

For Ar cluster irradiation the sample was introduced into a TOF.SIMS 5 by IONTOF (UHV conditions) at the Interdisciplinary Center of Analytics on the Nanoscale (ICAN) of the University of Duisburg-Essen, with the possibility to record time of flight (ToF) mass spectra simultaneously to irradiation. Ar_{5000} clusters with a kinetic energy of 5 keV were obtained by utilizing the integrated Gas Cluster Ion Beam (GCIB) source (see figure S3 for mass distribution). Mass spectra were recorded with a 30 keV Bi_3^+ ion beam to monitor the mass spectra intensities of organic compounds during the irradiation process. To prevent damage of graphene due to the Bi_3^+ ion beam the mass spectra were obtained on the SiO_2/Si substrate next to the graphene transistor. Both beams impact the sample at an angle of 45°.

3. Results and discussion

3.1. Exfoliated graphene

We will begin by discussing the adsorption and Raman signals of CoOEP on exfoliated graphene to demonstrate the enhancement of the CoOEP Raman signals and for later comparison to the results obtained for the graphene transistors. In figures 1(a) and (c) an AFM image and a Raman spectrum of an exfoliated graphene sample are shown. The AFM image reveals the typical clean surface of exfoliated graphene with only a few adsorbates visible. In the Raman spectrum the G- and 2D-mode of graphene can easily be identified and the absence of the D-mode indicates that the sample is practically free of defects because the D-mode originates from a resonant Raman scattering and an elastic scattering process at a defect [34–36]. After deposition of CoOEP onto the sample the AFM image reveals the formation of chain-like adsorbates with a length of 100 nm up to 200 nm (figure 1(b)), sometimes even more (see figure S2). The corresponding Raman spectrum in figure 1(d) displays a large number of additional modes which were not measured before deposition of the CoOEP molecules and can be unambiguously assigned to Raman modes known for CoOEP (see figure S1). The additional modes are quite dominant in the spectrum and even exceed the graphene Raman modes in terms of intensity. The G-mode of graphene is no longer identifiable since three strong CoOEP modes can be found around 1600 cm^{-1}. Since the AFM image in figure 1(b) demonstrates that the amount of molecules deposited onto the sample does not even lead to a full monolayer of molecules on the graphene surface, we conclude that the Raman signal of CoOEP is enhanced by the so called GERS [5]. To further emphasize this we want to point out that no CoOEP Raman signals can be detected in spectra taken from the surrounding SiO_2/Si substrate because of the low amount of molecules evaporated onto the sample. We therefore refrain from
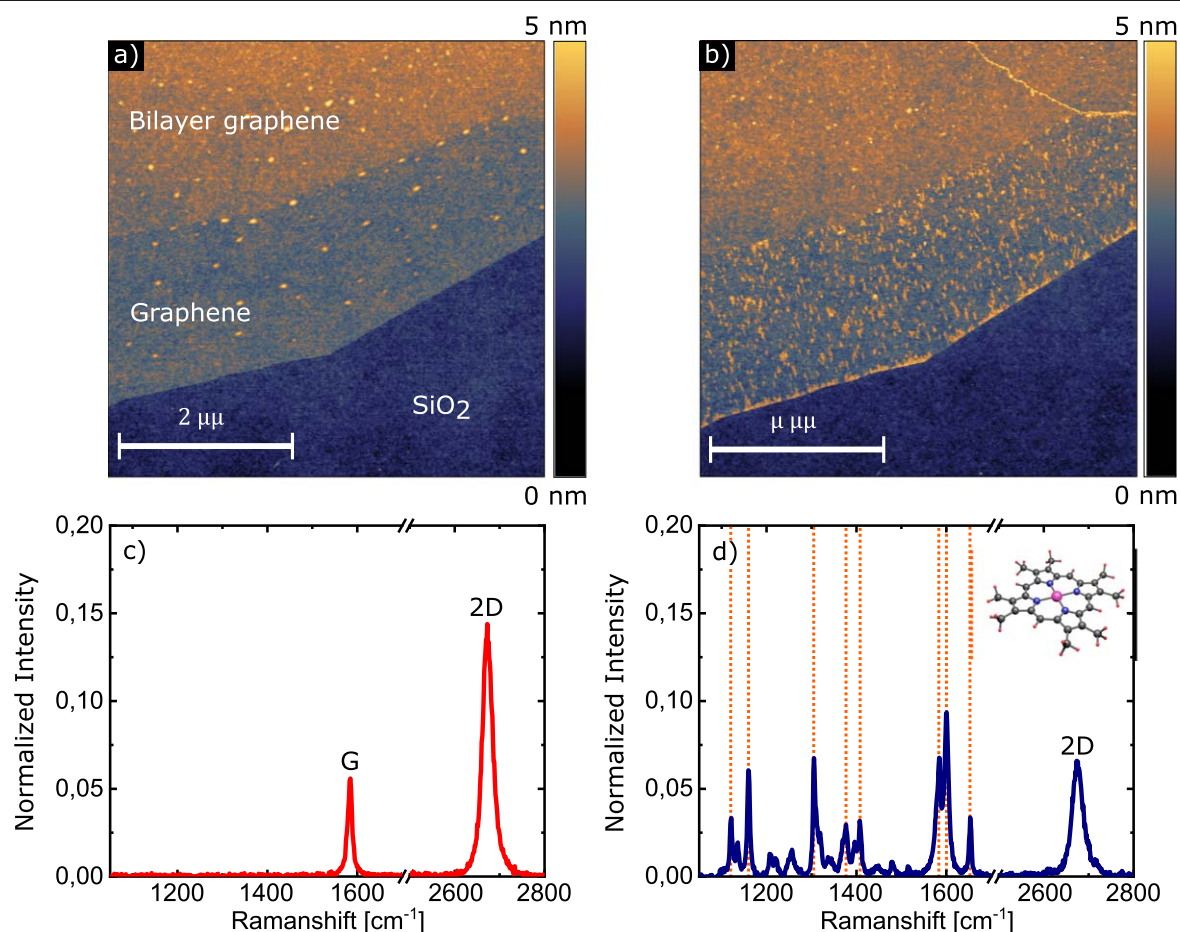
Figure 1. AFM images (a), (b) and Raman spectra (c), (d) of exfoliated graphene before and after deposition of CoOEP molecules showing features in the topography and the Raman spectrum (marked with the orange lines) of the samples after molecule deposition that can be attributed to the CoOEP molecules. The Raman spectra are normalized to the intensity of the silicon peak at 520 cm^{-1} stemming from the substrate.

calculating the enhancement factor for the CoOEP molecules which is usually defined by the intensity ratio between the molecular Raman signal on graphene and the molecular Raman signal on the substrate. In the work of Kim *et al* the enhancement factor for different metal-octaethylporphyrins (FeOEP and PtOEP), where only the Co atom in the center of the molecule is replaced by either a Fe or a Pt atom, is found to be 10-30 (depending on which mode is considered) [37]. We observe a rather small change in the peak position of the CoOEP Raman modes in comparison to the peak positions measured for CoOEP powder (see table 1 in SI (available online at stacks.iop.org/NANO/32/205702/mmedia)) indicating that there is a weak coupling between the molecules and graphene. Thus the molecules are basically physisorbed and both, graphene and CoOEP, remain chemically unchanged.

3.2. CVD graphene field-effect transistors

In the next step we fabricated graphene transistors, using CVD graphene, by the photolithography process described above. After CoOEP molecules were deposited onto these graphene transistors, CoOEP Raman modes can no longer be detected and there are no differences between the Raman

spectra measured before and after deposition of the molecules (figures 2(a), (b)). The small D-peak arising can be attributed to a small number of defects induced during the photo-lithography process. The AFM image in figure 2(c) shows the edge of the graphene channel of the transistor and reveals that large areas of graphene are covered with contaminations. By zooming in on the edge of the graphene channel (figure 2(d)) we find that the height of graphene is approximately 3.5 nm, which is around (2–2.5) nm higher than the typical value of graphene on top of a SiO$_2$/Si substrate measured by AFM [38]. These contaminations are most likely photoresist residues due to the lithography process and seem to cover large areas of the graphene channel in form of a closed layer. This resist layer prevents the direct adsorption of CoOEP molecules on the graphene surface. Therefore a charge transfer which is crucial for the chemical mechanism enabling GERS [18] cannot take place and as a consequence no CoOEP Raman modes can be detected in the spectra taken from the graphene transistors (figure 2(b)).

Residues remaining after a lithography step are a well known problem for graphene transistors and it has already been shown that standard solvents and removers can not completely remove these residues [39–41]. While for a
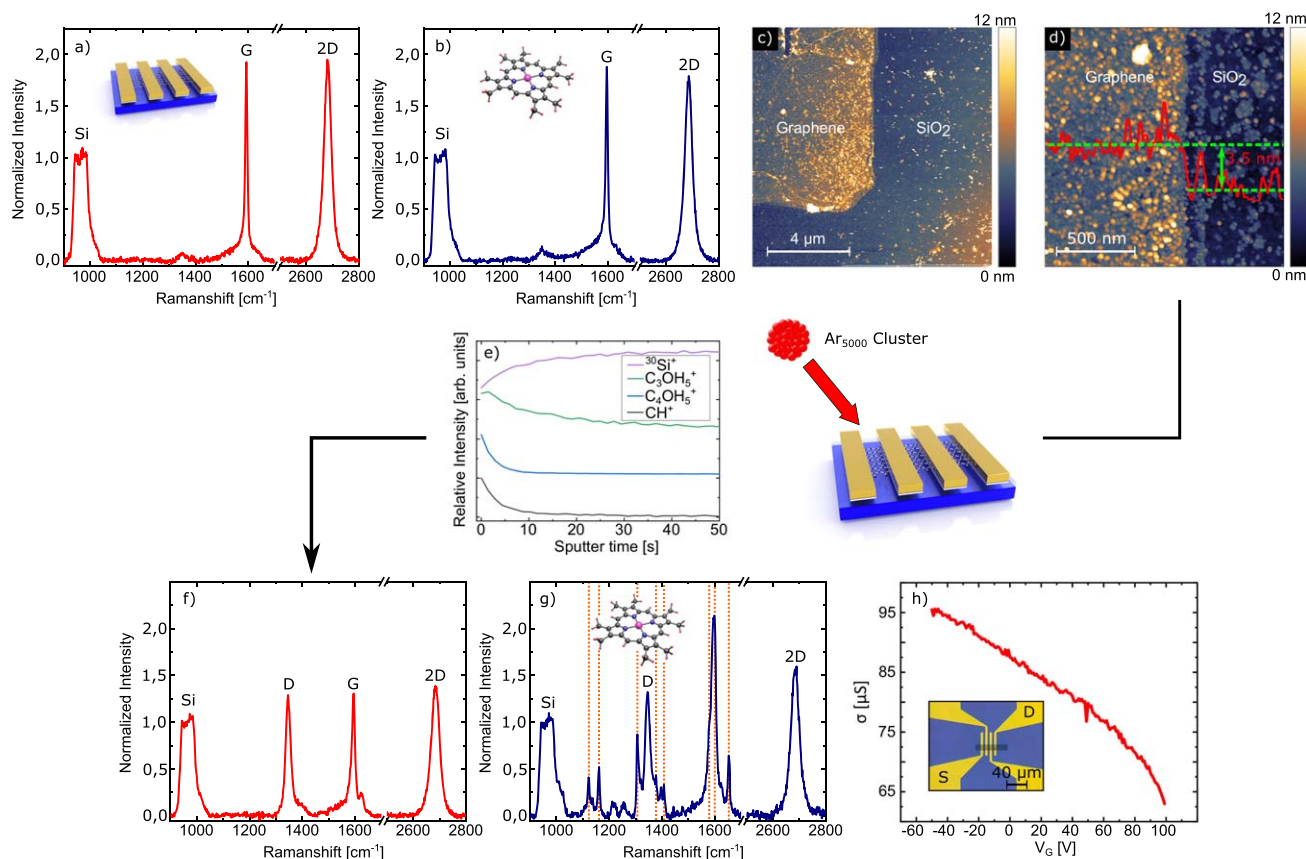
Figure 2. Raman, AFM and electrical characterization of the transistors based on CVD graphene. The Raman spectra before (a) and after (b) deposition of CoOEP molecules show no significant difference. (c) AFM image of the edge of the graphene transistor revealing large scale contaminations by resist residues on the graphene surface. (d) More detailed AFM image of the graphene edge demonstrating that the residues seem to form a closed layer. A linescan displays a height of approximately 3, 5 nm for graphene with respect to the substrate indicating that the residue layer is at least a few nm thick. (e) Secondary ion mass spectra taken during irradiation show that the signal intensities corresponding to various organic compounds diminish while the ^{30}Si signal of the surrounding substrate increases with increasing sputter time. The intensity of each compound is normalized to their respective signal at the beginning of the irradiation. The signals of the different compounds are offset to each other for a better overview. (f) After Ar cluster irradiation the D-peak of graphene arises indicating that defects are introduced into graphene by the irradiation. (g) After another deposition of CoOEP molecules clear Raman signals of the molecules can be measured in the Raman spectrum. (h) Electrical characterization after the molecular deposition step demonstrates p-doped behaviour of the transistor.

standard G-FET this may be still acceptable for a GERS device it is clearly not. In the following we will describe our approaches for tackling this problem. We begin with the results obtained for a 'classical' approach, i.e. by removing the residues after the photolithography process by particle bombardment. Tyler *et al* have demonstrated that a mass-selected Ar_{5000} ion cluster beam with a kinetic energy of 5 keV (which corresponds to an energy of 1 eV/atom) under an angle of 45° and a fluence of $5 \cdot 10^{14}$ ions cm^{-2} can remove poly(methyl methacrylate) from graphene without damaging the graphene too much [42]. We adapt this approach as it is especially suitable for large scale CVD-graphene-based processes because it is a lot faster than, e.g. cleaning graphene with an AFM in contact mode [43, 44] and can be applied to a large number of devices on the same wafer with almost no time needed for adjusting the setup. Compared to traditional Ar$^+$ ion bombardment for cleaning of surfaces, Ar Cluster ions have a much smaller kinetic energy per atom (in our case around 1eV/atom compared to ~keV for Ar$^+$ ions). This results in a larger sputter yield for organic resist

residues and a lower sputter yield for graphene [42]. Furthermore, the setup used in our work has the advantage that the Ar cluster ion source is integrated in a time of flight (ToF) mass spectrometer. This allows us to monitor the time of flight secondary ion mass spectra (SIMS) signal of organic compounds belonging to the resist residues during the cleaning process and therefore giving us detailed insights on the progress of the cleaning process. This is in particular helpful because the thickness of the residue layer may vary between different samples and processes. In addition to the SIMS data we carried out AFM and Raman measurements to investigate the effectiveness of the cleaning process and to monitor the influence of the procedure on the graphene transistors.

From the SIMS-spectra recorded during the cleaning process we can clearly conclude that different organic compounds are rapidly (on the time-scale of minutes) diminished while the ^{30}Si signal of the surrounding substrate increases, see figure 2(e). This indicates that the residual photoresist layer is indeed effectively removed by the cluster irradiation.

The AFM images of the irradiated graphene transistors support this finding as we can identify regions of free graphene surface in between some hillocks originating from remaining residues after the irradiation (see figure S4). Raman spectra of the graphene transistors after irradiation show a large D-peak (figure 2(f)), indicating that defects are now present in graphene [45–47, 4]. The formation of defects in graphene due to the irradiation with Ar cluster ions was already observed [42, 48] and is driven by the kinetic energy of the projectiles. Since the penetration depth of Ar cluster ions is in the range of around a few nm defects will be only introduced when the residues on graphene have been removed and the Ar cluster ions can interact directly with graphene. The inhomogeneity of the residue layer therefore leads to areas where all contaminations are removed during irradiation, while other areas remain covered. Within the cleaned areas, additional defects will be induced, while the areas still covered with residues are protected during irradiation. For sputter cleaning purposes typically the fluence is increased until the species to be removed is gone. For 3D materials, the unwanted consequences of this procedure such as sputter-induced defects can often be remedied by a subsequent annealing step, allowing atoms from the bulk to fill in the vacancies. However, in the case of a 2D material this technique appears inefficient for obvious reasons [49].

In combination, our SIMS, AFM, and Raman data confirm that irradiation by Ar cluster ions is indeed a suitable tool to remove contaminations from graphene typically present after photolithography. More importantly, after the post-processing step the devices are still fully functional as transistors and with respect to GERS as we will show in the following. After yet another evaporation step of CoOEP onto these irradiated graphene transistors, Raman enhancement of CoOEP can now be observed (figure 2(g)). When we compare the Raman spectrum in figure 2(g) to the Raman spectrum of CoOEP on exfoliated graphene (figure 1(d)) the first thing to notice is that the intensity of the Raman modes of CoOEP is smaller on the irradiated transistors, e.g. comparing the intensity ratio of the CoOEP modes to the 2D mode of graphene. This is not really surprising since the resist residues have not been completely removed by the irradiation and therefore parts of the graphene surface are still not available for molecular adsorption. Because the signal strength in GERS depends directly on the number of molecules in contact with the graphene surface [50] the resulting Raman signal of the molecules is reduced. Furthermore, parts of the CoOEP Raman spectrum overlap with the defect-activated D-mode of graphene around $1350 \, cm^{-1}$ and therefore some modes are not as clearly identifiable as in the spectrum in figure 1(d). Nevertheless a number of CoOEP modes is still identifiable and therefore accessible for characterization. Consequently, one has to deal with the compromise of hindered molecular adsorption because of photoresist residues on the one hand or a possible influence of defects on the adsorption behaviour and Raman enhancement on the other hand. The main influence of defects in graphene on GERS (for moderate defect densities) is the change of the doping level in graphene which modulates the Raman enhancement and can even lead to an increase of the molecular Raman signal [51, 52]. Because in a field-effect graphene transistor the doping level can be controlled by the gate voltage a possible influence of the defects on the molecular Raman signal could thus be compensated. The peak positions of the remaining CoOEP modes do not change significantly compared to the values obtained for exfoliated graphene (see table 1 in SI). This leads us to the conclusion that the interaction between the molecules and graphene is not strongly influenced by the number of defects induced during the irradiation.

To examine if graphene's Fermi level can still be tuned after the irradiation procedure we carried out field-effect dependent transport measurements. The transport characteristics (figure 2(h)) displays the expected behaviour of a p-doped graphene transistor with a decreasing conductivity when increasing the backgate voltage. Because of the large p-doping, the charge neutrality point is shifted to backgate voltages larger than 100 V. Graphene transistors can be p-doped by resist residues due to the photolithography process [53], but additionally our transfer process causes a strong p-doping of graphene even prior to processing [33]. Apart from the strong doping, figure 2(h) demonstrates that the transistor is still operational after the irradiation, meaning that it displays the typical electrical behavior of non-irradiated graphene transistors.

While the method presented above works surprisingly well, it comes along with the unavoidable disadvantages of all post-processing techniques based on particle bombardment. Particle irradiation will always introduce defects which may influence the Raman enhancement of the adsorbed molecules [51, 54, 55]. In addition, no irradiation-scheme will be able to remove the entire residue layer. This again presents a serious drawback, in particular if the fundamental interaction between graphene and CoOEP (or other molecules) is to be investigated and appears to be an issue which remains completely unaddressed in previous studies published on this topic [22–24]. In order to provide the cleanest interface possible one would ideally avoid the exposure of CoOEP/graphene to any of the lithography steps when fabricating the device. This is the key to the second approach to be presented in the following. The principle of our approach is to deposit CoOEP molecules onto a pristine CVD graphene (base) layer supported on a SiO_2/Si substrate and then to transfer a second CVD graphene layer (top layer) on top yielding a graphene/molecule/graphene heterostructure which is then processed further. The graphene top layer is expected to fully encapsulate and protect the CoOEP molecules adsorbed onto graphene as well as the graphene base layer itself from the harsh process steps of the photolithography. This protective functionality is inherent to graphene being impermeable to fluids like, e.g. water [56, 57]. While the idea seems straightforward its implementation is in fact not so trivial: the standard transfer method for the base layer cannot be used for the top layer again because the molecules are washed away from the base layer when trying to scoop up the top layer from its solvent. Therefore we developed a new technique as discussed in the following paragraph.

The principle of our novel stacking process is outlined in figures 3(a)–(d). We start with a CVD graphene sheet transferred onto a SiO$_2$/Si substrate (figure 3(a)). We want to recall that the transfer process used in this entire work takes place like described in the method section, i.e. without any need of an additional supportive polymer layer to stabilize the graphene sheet during the transfer [33]. As a consequence the molecules may adsorb directly onto the clean CVD graphene base layer without any prior treatment. After evaporation of the CoOEP molecules onto the base layer (figure 3(b)) a second CVD graphene sheet was prepared in the usual way, i.e. by etching the copper substrate in an ammonium persulfate (APS) solution (figure 3(c)) and replacing the APS solution with water. Subsequently the CVD graphene base layer with CoOEP molecules on top (from figure 3(b)) was carefully dipped *from above* onto the graphene sheet (the future top layer) floating on the water surface (figure 3(d)). This method effectively prevents the molecules from being washed away.

The success of such a process can be easily monitored by optical microscopy as shown in figure 3(d). The contrast of graphene increases by $\approx 2.3\%$ for every additional layer [58] and we can clearly distinguish three areas with different brightness which we assign to the bare SiO$_2$/Si substrate (brightest), base layer graphene (darker) and areas where the second graphene (top) layer was successfully transferred (darkest). The graphene top layer exhibits a lot more cracks in comparison to the base layer. This is due to the upside-down dipping process being rather harsh compared to the standard transfer technique of CVD graphene (scooping from below). Nevertheless, large areas of the sample (notice the scale bar) consist of the graphene/CoOEP/graphene heterostructure and areas of around $100 \times 100\,\mu$m with no cracks in the top graphene layer, suitable for transistor processing, can be easily found.

To investigate if the top graphene layer indeed effectively protects the CoOEP molecules and the underlying graphene base layer as expected, we took Raman spectra. In figure 4 the Raman spectrum of a CVD graphene base layer after evaporation of CoOEP molecules (a) and after the transfer of the top graphene layer (b) are shown. The spectrum in figure 4(b) is taken from areas with the lowest brightness in the corresponding optical image. Figure 4(c) shows the spectrum of a sample processed into a transistor by photolithography. The intensities of the Raman spectra shown in figure 4 are all normalized by the intensity of the silicon peak at around 520 cm^{-1} to enable us a rough comparison of the intensities. The CoOEP Raman modes can clearly be identified in all of these spectra and their intensities do not vanish after the photolithography step (figure 4(c)), which proves the protective functionality of the second graphene layer even under the harsh conditions during photolithography processing.

The graphene Raman modes (G- and 2D-mode) are stronger in the spectra recorded for the heterostructure (figures 4(b), (c)) which suggests that we are indeed measuring at locations where the top graphene layer is present. Furthermore we do not observe the defect associated D-mode of graphene after the photolithography process (figure 4(c)) so
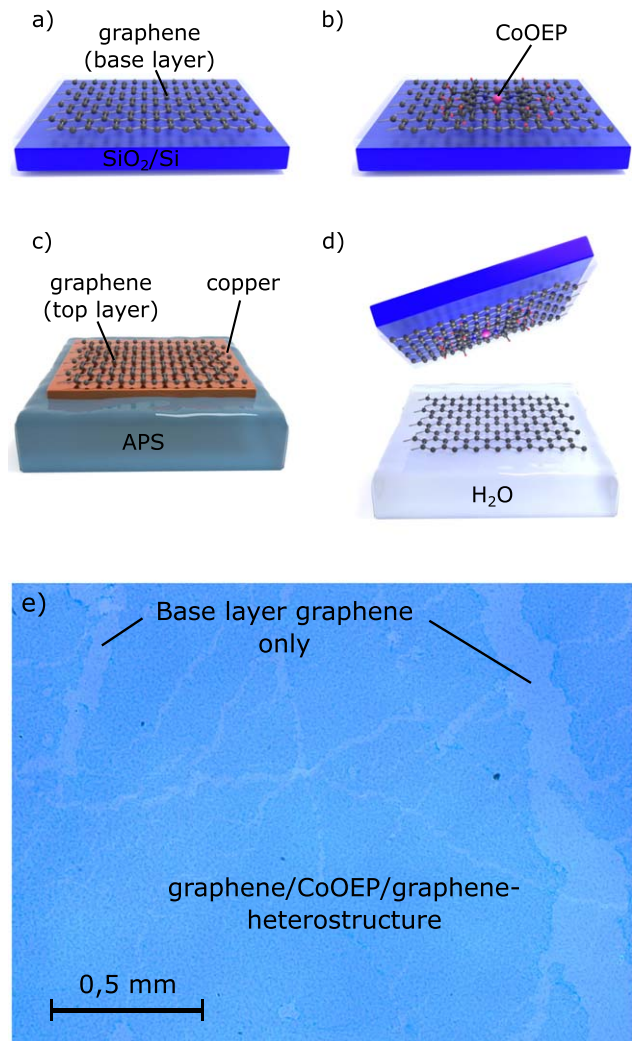

Figure 3. Schematic of the fabrication protocol and optical image of the resulting graphene/CoOEP/graphene heterostructure. (a) CVD graphene (base layer) is transferred onto a SiO$_2$/Si substrate as described in the text and CoOEP molecules are evaporated on top of it (b). (c) The second graphene (top) layer is prepared by etching the copper substrate in an ammonium persulfate solution. After the copper substrate is etched away the acid is replaced with water and the graphene sheet floating on top of the water is transferred to the already existing graphene base layer with CoOEP molecules (from (b)) by carefully dipping it from above onto it (d). As a result the areas with one layer or two layers graphene can be distinguished with an optical microscope because of their respective brightness (e). This approach leads to the formation of large areas of a graphene/CoOEP/graphene heterostructure.

that all CoOEP Raman modes can be identified clearly. The positions of the CoOEP Raman modes do not differ significantly compared to the values obtained for exfoliated and irradiated graphene transistors (see table 1 in SI) again demonstrating that the interaction between molecule and graphene is not influenced by the fabrication procedure.

Finally, we demonstrate that the transistor devices fabricated with our novel approach are fully functional and may be used for GERS experiments with controllable charge carrier concentration. In figure 4(d) we show the results of electrical transport measurements that we carried out to verify
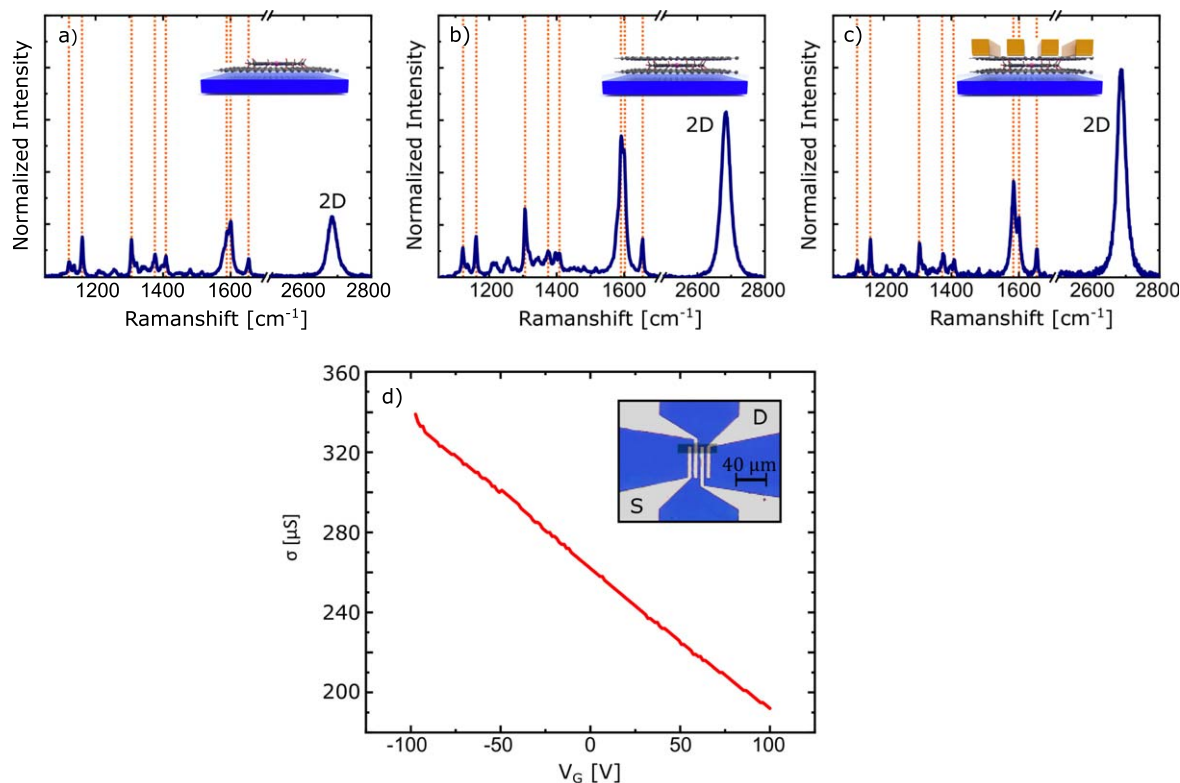
Figure 4. Raman spectra of different fabrication steps of the graphene/CoOEP/graphene heterostructure outlined in figure 3. (a) Raman spectrum of CVD graphene after deposition of CoOEP molecules. (b) Raman spectrum of the same sample after the transfer of the second graphene layer at a location where the fabrication of a graphene/CoOEP/graphene heterostructure was successful. (c) Raman spectrum of the graphene/CoOEP/graphene heterostructure after it has been processed to a field-effect transistor. In all spectra the CoOEP Raman modes are clearly visible demonstrating that the second graphene layer indeed protects the molecules during the photolithography process. All three spectra have been normalized to the intensity of the silicon mode at $520 \, cm^{-1}$. (d) Electrical characterization of the device indicating a p-doped graphene transistor with a charge neutrality point at backgate voltages larger than 100 V.

if it is possible to tune the Fermi level in such a graphene/CoOEP/graphene heterostructure. The transistor shows the behaviour of a highly p-doped graphene transistor with a charge neutrality point beyond 100 V backgate voltage. This result clearly demonstrates that it is possible to effectively control the charge carrier density in the graphene/CoOEP/graphene heterostructure field-effect device fabricated following the fabrication protocol as described above enabling a Fermi level dependent investigation of the enhanced CoOEP Raman signals. A major advantage of our approach is the cleanliness of the interface between the base graphene layer and the CoOEP molecules since the graphene base has never been exposed to any contaminations. Therefore this structure is ideal for studying the coupling between graphene and CoOEP by the means of GERS.

4. Conclusion

Graphene-enhanced Raman spectroscopy is a powerful technique for molecular detection. By using a graphene field-effect device as a substrate the unique possibility arises to investigate the nature of the GERS effect in great detail and to study the coupling between graphene and the adsorbed molecules by spectroscopic means. In our work we have

demonstrated that the Raman signals of CoOEP molecules which are an interesting candidate in the field of molecular spintronics, are enhanced by graphene as a substrate so that even submonolayer films of CoOEP can be investigated. By using CVD graphene for field-effect transistor fabrication we exploit processes compatible with industrial fabrication for the spectroscopical analysis of molecule graphene interactions. We have shown that residues stemming from the photolithography process necessary for transistor fabrication can hinder the charge transfer between molecules and graphene so that GERS is not taking place. We established irradiation with Ar_{5000} cluster ions as a fast, reproducible and compatible method to effectively remove these resist residues, a suitable method for FETs which require an active channel exposed to the environment, e.g. in molecular sensing devices. Enhanced Raman signals of CoOEP molecules can indeed be measured again after evaporating the molecules onto the irradiated transistors. The irradiation introduces a moderate number of defects into graphene but earlier studies have shown that graphene in general and also G-FETs in particular are quite resistant towards harsh conditions such as chemical attacks [59] or energetic ion irradiation [60–64]. We can further corroborate these findings since the transistor is still functional after the irradiation process. Furthermore we developed an alternative approach to solve the problem of

residues blocking the molecular adsorption by encapsulating the molecules between two pristine graphene layers (both transferred without an additional supportive polymer layer) before processing the heterostructure into a field-effect device. The second, top graphene layer effectively protects the molecules from any processing steps to follow and makes a subsequent cleaning process obsolete. Because of the unique protective properties of graphene, such devices cannot only be studied for extended periods of time but can also be easily exchanged between different experimental setups (or groups) to obtain comprehensive data from the same sample and to establish measurement standards. We have shown that in both cases functional transistors can be obtained behaving like highly p-doped graphene field-effect devices. Both approaches are applicable to various molecules and therefore our work marks a big step forward towards the investigation of a graphene/molecule hybridsystem by Raman spectroscopy under effective charge carrier control.

Acknowledgments

ORCID iDs

Stephan Sleziona ● https://orcid.org/0000-0003-2844-1134
Erik Pollmann ● https://orcid.org/0000-0002-3961-0426
Lukas Madauß ● https://orcid.org/0000-0003-2556-5967
Axel Lorke ● https://orcid.org/0000-0002-0405-7720
Heiko Wende ● https://orcid.org/0000-0001-8395-3541
Marika Schleberger ● https://orcid.org/0000-0002-5785-1186

References

[1] Novoselov K S, Geim A K, Morozov S V, Jiang D, Zhang Y, Dubonos S V, Grigorieva I V and Firsov A A 2004 Electric field effect in atomically thin carbon films *Science* **306** 666–9

[2] Ferrari A C *et al* 2006 raman spectrum of graphene and graphene layers *Phys. Rev. Lett.* **97** 187401

[3] Das A *et al* 2008 monitoring dopants by raman scattering in an electrochemically top-gated graphene transistor *Nat. Nanotechnol.* **3** 210–5

[4] Lucchese M M, Stavale F, Ferreira E M, Vilani C, Moutinho M, Capaz R B, Achete C A and Jorio A 2010 Quantifying ion-induced defects and raman relaxation length in graphene *Carbon* **48** 1592–7

[5] Ling X, Xie L, Fang Y, Xu H, Zhang H, Kong J, Dresselhaus M S, Zhang J and Liu Z 2010 Can graphene be used as a substrate for raman enhancement? *Nano Lett.* **10** 553–61

[6] Silver A, Kitadai H, Liu H, Granzier-Nakajima T, Terrones M, Ling X and Huang S 2019 Chemical and bio sensing using graphene-enhanced raman spectroscopy *Nanomaterials* **9** 516

[7] Xu W, Ling X, Xiao J, Dresselhaus M S, Kong J, Xu H, Liu Z and Zhang J 2012 Surface enhanced raman spectroscopy on a flat graphene surface *Proc. Natl. Acad. Sci. USA* **109** 9281–6

[8] Ling X, Wu J, Xu W and Zhang J 2012 Probing the effect of molecular orientation on the intensity of chemical enhancement using graphene-enhanced raman spectroscopy *Small* **8** 1365–72

[9] Xu W, Mao N and Zhang J 2013 Graphene: a platform for surface-enhanced raman spectroscopy *Small* **9** 1206–24

[10] Schlücker S 2014 Surface-enhanced raman spectroscopy: Concepts and chemical applications *Angew. Chem. Int. Ed.* **53** 4756–95

[11] Kneipp K, Moskovits M and Kneipp H 2006 *Surface-Enhanced Raman Scattering: Physics and Applications* (Berlin: Springer)

[12] Le F, Brandl D W, Urzhumov Y A, Wang H, Kundu J, Halas N J, Aizpurua J and Nordlander P 2008 Metallic nanoparticle arrays: A common substrate for both surface-enhanced raman scattering and surface-enhanced infrared absorption *ACS Nano* **2** 707–18

[13] Hao Q, Juluri B K, Zheng Y B, Wang B, Chiang I-K, Jensen L, Crespi V, Eklund P C and Huang T J 2010 Effects of intrinsic fano interference on surface enhanced raman spectroscopy: comparison between platinum and gold *J. Phys. Chem.* C **114** 18059–66

[14] Otto A, Mrozek I, Grabhorn H and Akemann W 1992 Surface-enhanced Raman scattering *J. Phys.: Condens. Matter* **4** 1143

[15] Blackie E J, Le Ru E C and Etchegoin P G 2009 Single-molecule surface-enhanced raman spectroscopy of nonresonant molecules *J. Am. Chem. Soc.* **131** 14466–72

[16] Otto A 2005 The chemical' (electronic) contribution to surface-enhanced raman scattering *J. Raman Spectrosc.* **36** 497–509

[17] Jiang X and Campion A 1987 Chemical effects in surface-enhanced raman scattering: Pyridine chemisorbed on silver adatoms on rh (100) *Chem. Phys. Lett.* **140** 95–100

[18] Ling X, Moura L G, Pimenta M A and Zhang J 2012 Charge-transfer mechanism in graphene-enhanced raman scattering *J. Phys. Chem.* C **116** 25112–8

[19] Ling X and Zhang J 2010 First-layer effect in graphene-enhanced raman scattering *Small* **6** 2020–5

[20] Valeš V, Kovaříček P, Fridrichová M, Ji X, Ling X, Kong J, Dresselhaus M S and Kalbáč M 2017 Enhanced raman scattering on functionalized graphene substrates *2D Mater.* **4** 025087

[21] Rana F 2008 "Graphene terahertz plasmon oscillators *IEEE Trans. Nanotechnol.* **7** 91–9

[22] Xu H, Xie L, Zhang H and Zhang J 2011 Effect of graphene fermi level on the raman scattering intensity of molecules on graphene *ACS Nano* **5** 5338–44

[23] Xu H, Chen Y, Xu W, Zhang H, Kong J, Dresselhaus M S and Zhang J 2011 Modulating the charge-transfer enhancement in gers using an electrical field under vacuum and an n/p-doping atmosphere *Small* **7** 2945–52

[24] Hao Q, Morton S M, Wang B, Zhao Y, Jensen L and Jun Huang T 2013 Tuning surface-enhanced raman scattering from graphene substrates using the electric field effect and chemical doping *Appl. Phys. Lett.* **102** 11102

[25] Bogani L and Wernsdorfer W 2008 Molecular spintronics using single-molecule magnets *Nat. Mater.* **7** 179–86

[26] Guo C S, Sun L, Hermann K, Hermanns C F, Bernien M and Kuch W 2012 X-ray absorption from large molecules at metal surfaces: Theoretical and experimental results for co-oep on ni(100) *J. Chem. Phys.* **137** 194703

[27] Farberovich O V and Mazalova V L 2016 Ultrafast quantum spin-state switching in the co-octaethylporphyrin molecular magnet with a terahertz pulsed magnetic field *J. Magn. Magn. Mater.* **405** 169–73

[28] Hermanns C F, Tarafder K, Bernien M, Krüger A, Chang Y-M, Oppeneer P M and Kuch W 2013 Magnetic coupling of porphyrin molecules through graphene *Adv. Mater.* **25** 3473–7

[29] Klar D *et al* 2014 field-regulated switching of the magnetization of co-porphyrin on graphene *Phys. Rev.* B **89** 144411

[30] Kirkpatrick A 2003 Gas cluster ion beam applications and equipment *Nucl. Instrum. Methods Phys. Res.* B **206** 830–7

[31] Bae S *et al* 2010 Roll-to-roll production of 30-inch graphene films for transparent electrodes *Nat. Nanotechnol.* **5** 574

[32] Li X *et al* 2009 Large-area synthesis of high-quality and uniform graphene films on copper foils *Science* **324** 1312–4

[33] Madauß L *et al* 2020 a swift technique to hydrophobize graphene and increase its mechanical stability and charge carrier density *NPJ 2D Mater. Appl.* **4** 11

[34] Tuinstra F and Koenig J L 1970 Raman spectrum of graphite *J. Chem. Phys.* **53** 1126–30

[35] Ferrari A C and Robertson J 2000 Interpretation of raman spectra of disordered and amorphous carbon *Phys. Rev.* B **61** 14095–107

[36] Ferrari A C and Basko D M 2013 Raman spectroscopy as a versatile tool for studying the properties of graphene *Nat. Nanotechnol.* **8** 235–46

[37] Kim B-H, Kim D, Song S, Park D, Kang I-S, Jeong D H and Jeon S 2014 Identification of metalloporphyrins with high sensitivity using graphene-enhanced resonance raman scattering *Langmuir* **30** 2960–7

[38] Akcöltekin S, El Kharrazi M, Köhler B, Lorke A and Schleberger M 2009 Graphene on insulating crystalline substrates *Nanotechnology* **20** 155601

[39] Ishigami M, Chen J H, Cullen W G, Fuhrer M S and Williams E D 2007 Atomic structure of graphene on SiO$_2$ *Nano Lett.* **7** 1643–8

[40] Cheng Z, Zhou Q, Wang C, Li Q, Wang C and Fang Y 2011 Toward intrinsic graphene surfaces: A systematic study on thermal annealing and wet-chemical treatment of SiO$_2$-supported graphene devices *Nano Lett.* **11** 767–71

[41] Lin Y-C, Lu C-C, Yeh C-H, Jin C, Suenaga K and Chiu P-W 2012 Graphene annealing: how clean can it be? *Nano Lett.* **12** 414–9

[42] Tyler B J, Brennan B, Stec H, Patel T, Hao L, Gilmore I S and Pollard A J 2015 Removal of organic contamination from graphene with a controllable mass-selected argon gas cluster ion beam *J. Phys. Chem.* C **119** 17836–41

[43] Lindvall N, Kalabukhov A and Yurgens A 2012 Cleaning graphene using atomic force microscope *J. Appl. Phys.* **111** 064904

[44] Choi W, Shehzad M A, Park S and Seo Y 2017 Influence of removing pmma residues on surface of cvd graphene using a contact-mode atomic force microscope *RSC Adv.* **7** 6943–9

[45] Ferrari A C 2007 Raman spectroscopy of graphene and graphite: Disorder, electron-phonon coupling, doping and nonadiabatic effects *Solid State Commun.* **143** 47–57

[46] Cançado L G *et al* 2011 quantifying defects in graphene via raman spectroscopy at different excitation energies *Nano Lett.* **11** 3190–6

[47] Dresselhaus M S, Jorio A, Souza Filho A G and Saito R 2010 Defect characterization in graphene and carbon nanotubes using raman spectroscopy *Phil. Trans. R. Soc.* A **368** 5355–77

[48] Kim S *et al* 2018 multi-purposed ar gas cluster ion beam processing for graphene engineering *Carbon* **131** 142–8

[49] Schleberger M and Kotakoski J 2018 2d material science: defect engineering by particle irradiation *Mater* **11** 1885

[50] Ling X and Zhang J 2010 First-Layer Effect in Graphene-Enhanced Raman Scattering *Small* **6** 2020–5

[51] Huh S, Park J, Kim Y S, Kim K S, Hong B H and Nam J-M 2011 Uv/ozone-oxidized large-scale graphene platform with large chemical enhancement in surface-enhanced raman scattering *ACS Nano* **5** 9799–806

[52] Feng S, Dos Santos M C, Carvalho B R, Lv R, Li Q, Fujisawa K, Elías A L, Lei Y, Perea-López N, Endo M, Pan M, Pimenta M A and Terrones M 2016 Ultrasensitive molecular sensor using n-doped graphene through enhanced raman scattering *Sci. Adv.* **2** e1600322

[53] Pirkle A, Chan J, Venugopal A, Hinojos D, Magnuson C W, McDonnell S, Colombo L, Vogel E M, Ruoff R S and Wallace R M 2011 The effect of chemical residues on the physical and electrical properties of chemical vapor deposited graphene transferred to SiO$_2$ *Appl. Phys. Lett.* **99** 122108

[54] Feng S, Lin Z, Gan X, Lv R and Terrones M 2017 Doping two-dimensional materials: Ultra-sensitive sensors, band gap tuning and ferromagnetic monolayers *Nanoscale Horiz.* **2** 72–80

[55] Kong X and Chen Q 2012 The positive influence of boron-doped graphene with pyridine as a probe molecule on sers: a density functional theory study *J. Mater. Chem.* **22** 15336

[56] Berry V 2013 Impermeability of graphene and its applications *Carbon* **62** 1–10

[57] Nilsson L, Andersen M, Balog R, Lægsgaard E, Hofmann P, Besenbacher F, Hammer B, Stensgaard I and Hornekær L 2012 Graphene coatings: Probing the limits of the one atom thick protection layer *ACS Nano* **6** 10258–66

[58] Nair R R, Blake P, Grigorenko A N, Novoselov K S, Booth T J, Stauber T, Peres N M R and Geim A K 2008 Fine structure constant defines visual transparency of graphene *Science* **320** 1308

[59] Miranda A and Lorke A 2018 Stability of suspended monolayer graphene membranes in alkaline environment *Mater. Res. Lett* **6** 49–54

[60] Ochedowski O, Lehtinen O, Kaiser U, Turchanin A, Ban-d'Etat B, Lebius H, Karlušić M, Jakšić M and Schleberger M 2015 Nanostructuring graphene by dense electronic excitation *Nanotechnology* **26** 465302

[61] Hopster J, Kozubek R, Ban-d'Etat B, Guillous S, Lebius H and Schleberger M 2014 Damage in graphene due to electronic excitation induced by highly charged ions *2D Mater.* **1** 011011

[62] Gruber E *et al* 2016 Ultrafast electronic response of graphene to a strong and localized electric field *Nat. Commun.* **7** 13948

[63] Ernst P, Kozubek R, Madauß L, Sonntag J, Lorke A and Schleberger M 2016 Irradiation of graphene field effect transistors with highly charged ions, *Nucl. Instrum. Methods* B **382** 71–5

[64] Ochedowski O, Marinov K, Wilbs G, Keller G, Scheuschner N, Severin D, Bender M, Maultzsch J, Tegude F J and Schleberger M 2013 Radiation hardness of graphene and MoS$_2$ field effect devices against swift heavy ion irradiation *J. Appl. Phys.* **113** 214306